Supplementary Table 1

Gene	Probe	Med_NSCLC	Med_NL	T test	Logrank overall	Logrank relapse free	Pathway
CERS6	AA758229_r_271	0.25	-0.32	8.40E-06	0.006	0.012	de novo synthesis
SMPD2	A_23_P82159	0.21	0.52	6.58E-04	0.11	0.084	Sphingomyelin
DEGS1	A_23_P126186	-0.16	-0.07	0.145	0.115	0.031	de novo synthesis
SMPD3	A_23_P152186	0.12	0.11	0.375	0.118	0.415	Sphingomyelin
GBA2	A_23_P18672	-0.11	-0.33	0.018	0.131	0.011	HexCer (GlcCer)
CERS4	A_23_T8322	0.13	0.13	0.328	0.15	0.215	de novo synthesis
SPTLC1	A_23_P43326	0.29	0.49	1.40E-04	0.154	0.321	de novo synthesis
SMPD1	A_23_P203488	-0.25	1.46	2.45E-04	0.18	0.576	Sphingomyelin
PHCA	A_23_P203665	0.13	0.14	0.917	0.218	0.136	S1P
CERS1	A_23_T30909	-0.51	-0.39	0.365	0.259	0.461	de novo synthesis
TMEM23	A_23_P115616	0.36	0.39	0.113	0.296	0.631	Sphingomyelin
CERK	A_23_P211659	-0.02	-0.26	0.006	0.331	0.474	C1P
TMEM23	A_23_P149791	0.1	0.85	0.073	0.339	0.585	Sphingomyelin
UGT8	A_23_P61346	-0.74	-1.52	0.003	0.368	0.315	HexCer (GalCer)
CERS3	A_23_T5195	0.16	0.05	0.041	0.455	0.483	de novo synthesis
GALC	A_23_P25964	0.16	0.93	0.001	0.457	0.695	HexCer (GalCer)
GCS	A_23_P123645	-0.7	-0.2	0.087	0.46	0.743	HexCer (GlcCer)
TMEM23	AK026683_2141	0.07	0.21	3.92E-04	0.554	0.543	Sphingomyelin
SMPD3	A_23_P163567	-0.93	-1.01	0.012	0.701	0.969	Sphingomyelin
SPTLC2	A_23_P3146	0.33	0.89	0.012	0.721	0.808	de novo synthesis
CERS1	A_23_T8203	0.86	1.33	2.15E-04	0.741	0.734	de novo synthesis
GBA3	A_23_P216536	0	0.13	0.017	0.761	0.355	HexCer (GlcCer)
SPHK1	A_23_P38106	-0.38	0.02	0.018	0.775	0.553	S1P
CERS2	A_23_T810	-0.05	0.14	0.048	0.816	0.92	de novo synthesis
ASAH2	A_23_P161171	-0.35	-0.65	0.003	0.89	0.812	S1P
UGT8	A_23_P72747	-1.06	-2.31	2.77E-04	0.943	0.867	HexCer (GalCer)
SPHK2	A_23_P208719	-0.46	-0.21	1.46E-05	0.955	0.445	S1P
CERS5	A_23_T4171	-0.08	-0.1	0.835	0.979	0.847	de novo synthesis

Altered ceramide metabolic gene expression in cancer tissues

Gene expression levels in ceramide metabolic pathways were compared among 149 NSCLC specimens and 5 normal lung mixtures. Genes with background levels or those without detection probes on the chip are not shown. *CERS6* expression level was associated with both overall and relapse-free survival. S1P, sphingosine-1-phosphate; C1P, ceramide-1-phosphate; HexCer, monohexosylceramide: GalCer, galactosylceramide; GlcCer, glucosylceramide.

Supplementary Table 2

Immunohistochemical expression of CERS6 in NSCLC and normal lung specimens

Lung Specimen(Lx)	Cancer	Normal lung	
		Type II pneumocyte	Pseudo-stratified ciliated epithelium
AD (L1)	2	0	0
AD (L2)	1	0	0
AD (L3)	2	0	0
AD (L4)	1	0	0
AD (L5)	1	0	0
AD (L6)	1	0	0
AD (L7)	2	0	1
AD (L8)	1	0	0
AD (L9)	2	0	0
AD (L10)	0	0	0
AD (L11)	1	0	0
AD (L12)	0	0	0
AD (L13)	1	0	0
AD (L14)	1	0	0
SCC (L15)	2	0	0
SCC (L16)	2	0	0
SCC (L17)	2	0	0
SCC (L18)	2	0	0
SCC (L19)	0	0	0
SCC (L20)	2	0	0
SCC (L21)	2	0	1
SCC (L22)	2	0	0
SCC (L23)	2	0	0
SCC (L24)	1	0	0
SCC (L25)	2	0	0
SCC (L26)	2	0	0
SCC (L27)	1	0	0

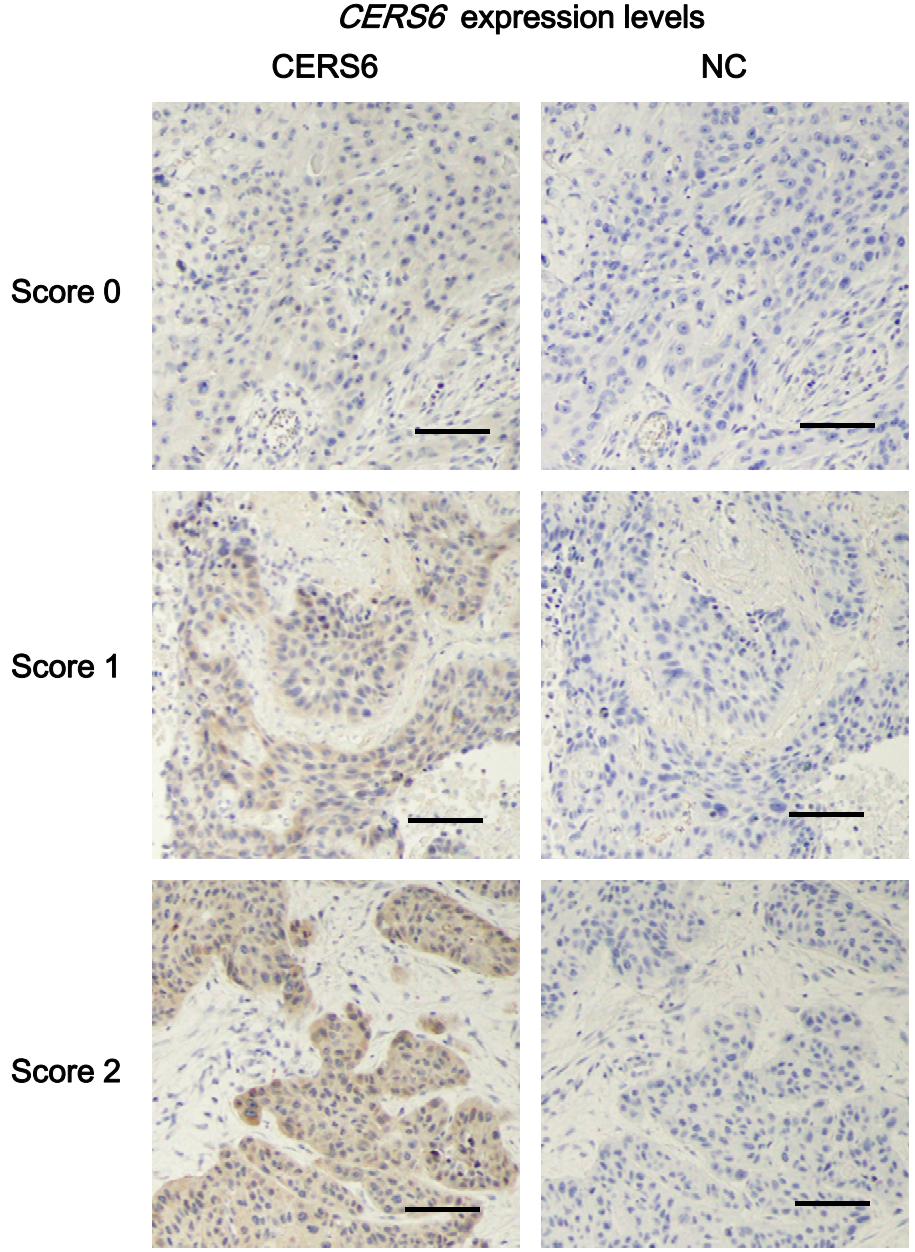

CERS6 protein highly expressed in NSCLC specimens.

Formalin-fixed paraffin sections were subjected to an immunoperoxidase study using an avidin-biotin peroxidase complex method. The CERS6 monoclonal antibody was used after antigen retrieval following microwave oven heating treatment. IHC stained slides were interpreted and scored on a scale ranging from 0 to 2, with samples with a staining score of 0 considered negative, and that of 1 and 2 weakly and strongly positive, respectively. Examples are shown in the right panels. AD, adenocarcinoma; SCC, squamous cell carcinoma. Bar, 0.2 mm.

Supplementary Table 3

Experiment	Name	Sequence
Luciferase vector construction	CERS6 WT-3'UTR F	ATCGATCTGAGTCTAGACTCCTGCTCCATGGATGATT
	CERS6 WT-3'UTR R	ATCGATCGAGGGGCCCGCAATTTCAAAATGGGCACT
	CERS6 MUT-3'UTR F	CAGTATTTGCATTTGGTCTTAGAATATTA
	CERS6 MUT-3'UTR R	TAATATTCTAAGACCAAATGCAAATACTG
	CERS6 WT-3'UTR seqF	CTCCTGCTCCATGGATGATT
	CERS6 WT-3'UTR seqR	GCAATTTCAAAATGGGCACT
siRNA (forward sequence only)	CERS5 siRNA-1	r(CAAGUAUCCUGAUAAGAAA)dTdT
	CERS5 siRNA-2	r(GGAGUAUCAAAGAAGCAAA)dTdT
	CERS6 siRNA-1	r(AAGGUCUUCACUGCAAUUACA)dTdT
	CERS6 siRNA-2	r(CAACUGACCUUCACUACUA)dTdT
	CERS6 siRNA-3	r(GUGUGArCUCCUGUUUGUU)dTdT
sh construct (forward sequence only)	CERS6 shRNA-2	GCAGGCCAATGGACCACAAATTCtcgaGAATTTGTGGTCCATTGGCC TGTTTTTT
	CERS6 shRNA-3	GCGGACGAACTAGGTGTTTAATCtcgaGATTAAACACCTAGTTCGTC CGTTTTTT
Real-time PCR	CERS5 F1	GTTCTGGGACATCCGACAGT
	CERS5 R1	CCAATAGAAGGCCAATTCCA

Supplementary Table 4

Precursor ion *m/z* (Q1)	Product ion *m/z* (Q3)
538.5	264.5
562.7	264.5
562.7	265.4
562.7	287.5
562.7	288.5
563.7	264.5
563.7	264.5
563.7	288.5
563.7	289.5
564.7	264.5
564.7	265.4
564.7	289.5
564.7	290.6
565.7	264.5
565.7	265.4
565.7	290.6
565.7	291.6
592.9	291.6

Supplementary Fig. 1

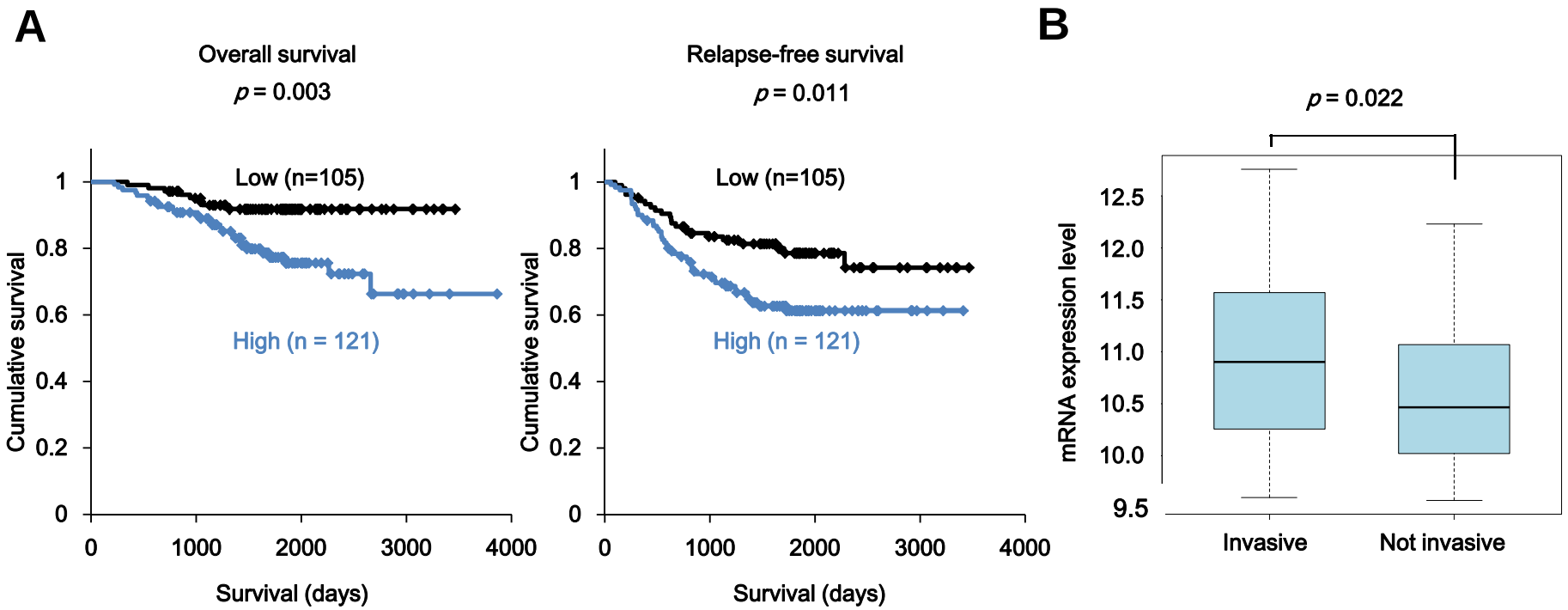

***CERS6* expression in breast cancer specimens.**
(A) Kaplan-Meier analysis of mRNA expression level of *CERS6* and prognosis (data from Cancer Res 2012;72:100-111). The high and low groups were classified by *CERS6* expression level relative to the median value. Cases lacking clinical information were omitted from the analysis. (B) Box plot analysis showing mRNA expression levels of *CERS6* and invasiveness. Using a breast cancer data set (J Natl Cancer Inst. 2011;103:264-72), *CERS6* expression levels were plotted into the 'Invasive' (n=69), and 'Not invasive' groups (n=28). *p* values were calculated using a two-tailed t test.

Supplementary Fig. 2

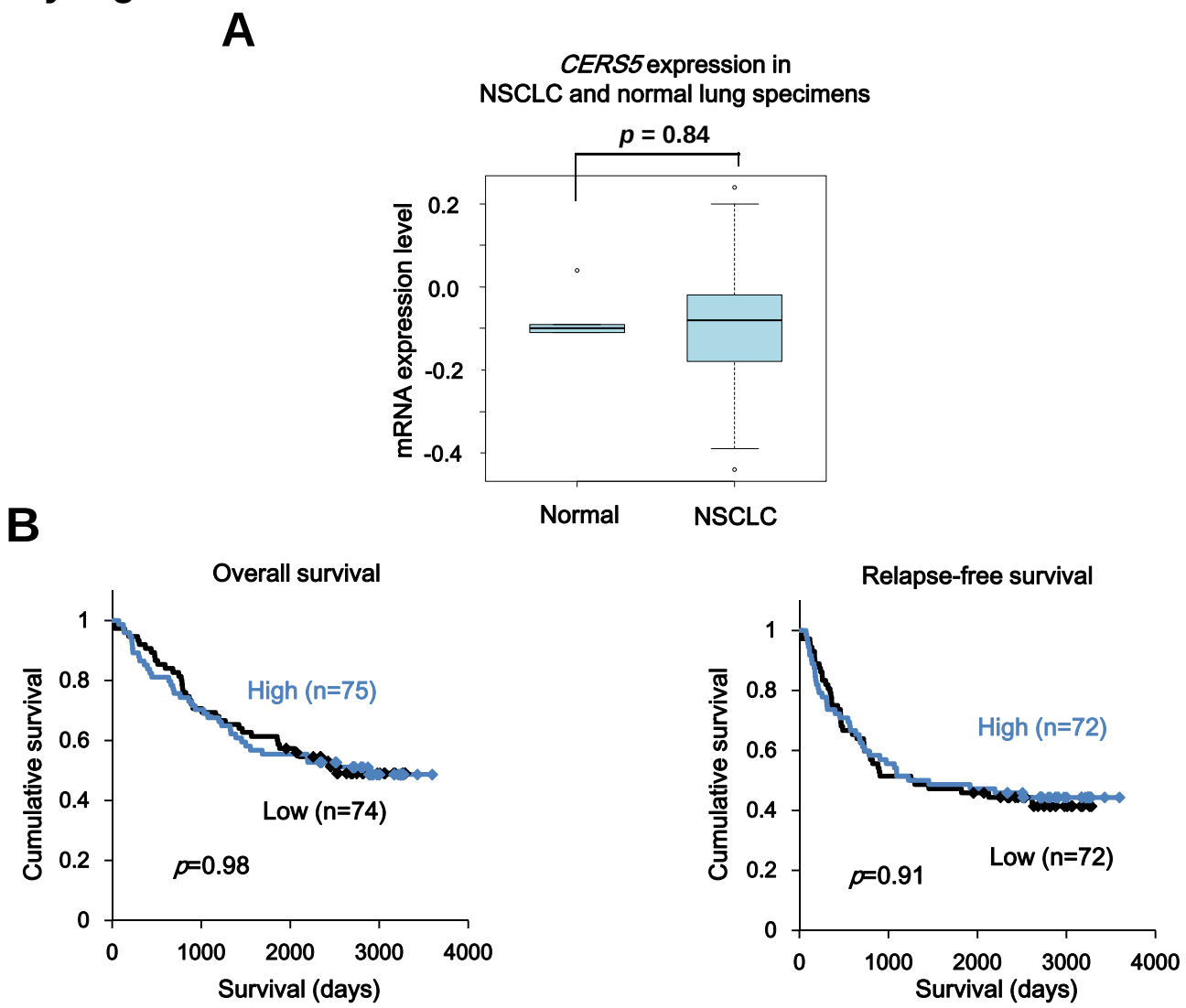

***CERS5* expression in NSCLC and normal specimens.**
(A) Box plot analysis of mRNA expression levels of *CERS5* in the 141 NSCLC and normal tissues. Normal, 5 normal lung mixtures; NSCLC, 141 cases. (B) Kaplan-Meier analysis showing overall survival (high and low, 74 and 75 cases, respectively) and relapse-free survival (high and low, 72 and 72 cases, respectively) curves in the 149 NSCLC cases. The high and low groups were classified based on *CERS5* expression levels relative to the median value.

Supplementary Fig. 3

A

Predicted miRNAs targeting *CERS6*

miRNA family	Context+ score	miRanda	Detection
hsa-miR-34a	-0.41	Y	Y
hsa-miR-217	-0.26	Y	N
hsa-miR-101	-0.23	Y	Y
hsa-miR-183	-0.17	Y	Y
hsa-miR-148a	-0.19	Y	Y
hsa-miR-200c	-0.10	Y	Y

B

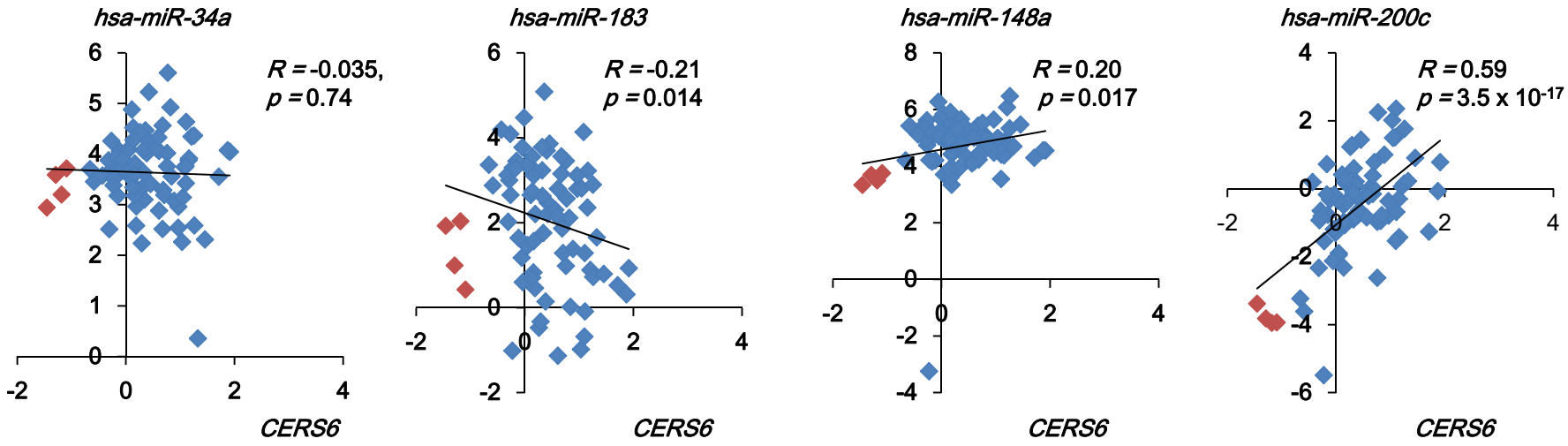

miRNA quantification using clinical specimens.
(A) Putative *CERS6*-targeting miRNAs were picked up using the prediction algorithms TargetScanHuman (Release 6.2) and miRanda. Conserved miRNAs were sorted according to the Context+ Score (TargetScanHuman). (B) Expression levels of the top 6 miRNAs in 79 adenocarcinoma (blue) and 4 normal (red) specimens were determined (Carcinogenesis 35; 2224-2231: 2014). In addition to *miR-101* (Fig. 2), sufficient expression levels of *miR-34a*, *miR-183*, *miR-148a*, *miR-200c*, but not *miR-217*, were observed.

Supplementary Fig. 4

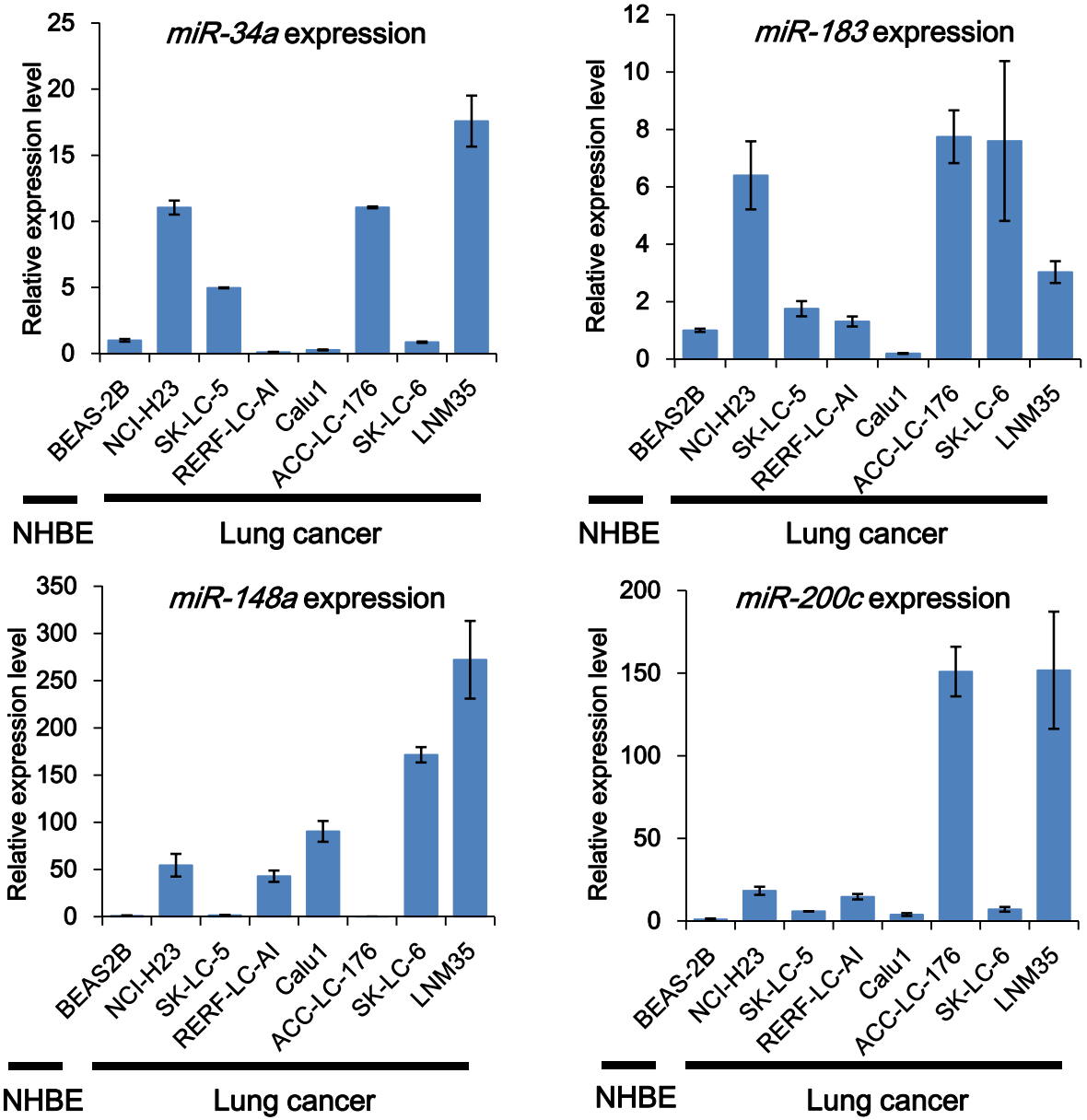

miRNA quantification using cell lines.

(A) Relative expression levels *of miR-34a, miR-183, miR-148a,* and *miR-200c* in a normal human bronchial epithelial cell line (NHBE) BEAS-2B and a panel of lung cancer cell lines were determined by quantitative RT-PCR. Bars, mean ± SD (n=3).

Supplementary Fig. 5

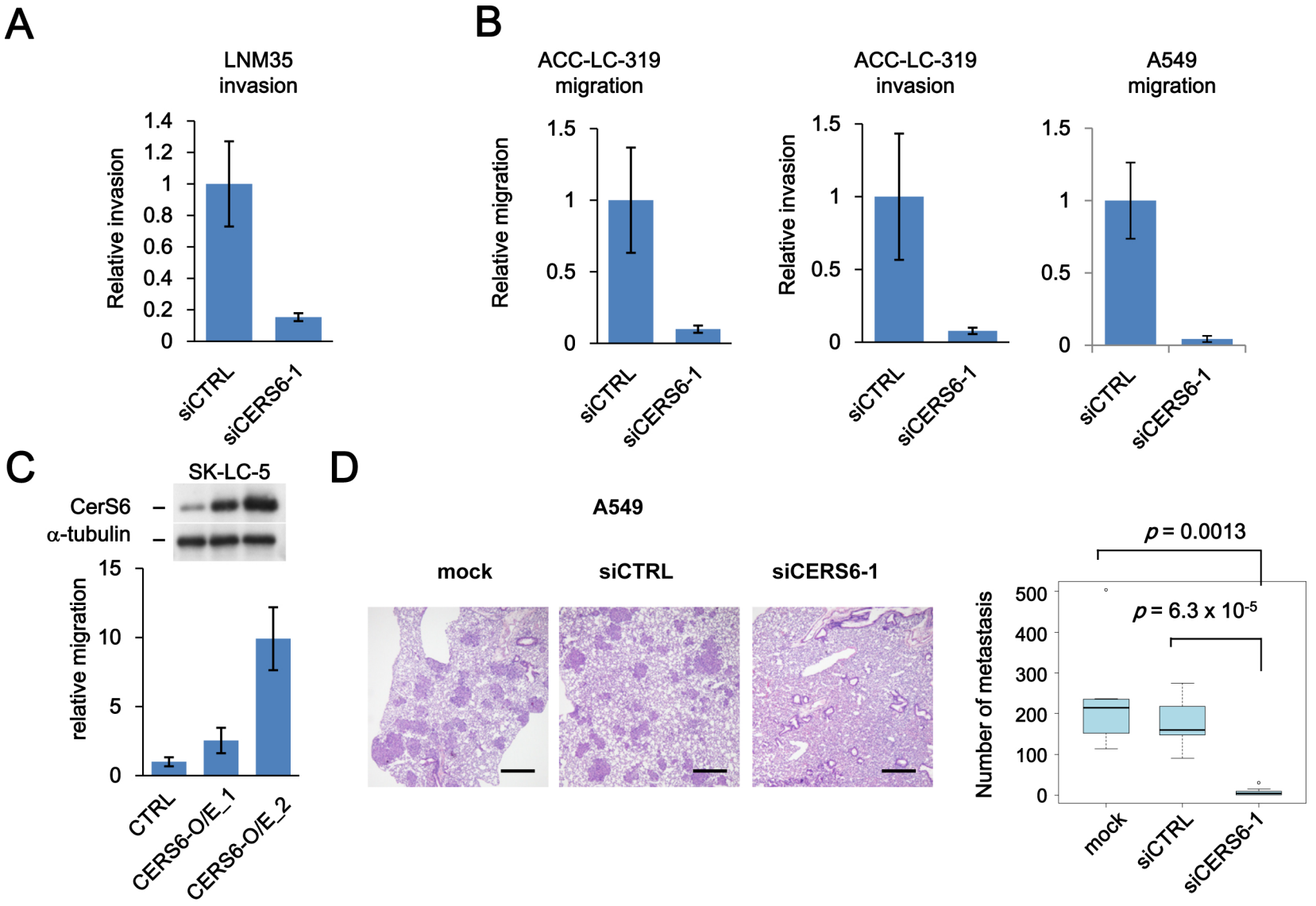

Knockdown of CERS6 suppresses lung cancer metastasis.

(A) Invasion assay to determine effects of CERS6 knockdown in LNM35 cells. CTRL, negative control siRNA; siCERS6-1, siRNA targeting *CERS6*. Bars, mean ± SD (n=3). (B) Migration and invasion assays were performed using ACC-LC-319 or A549 cells (n=4). (C) Migration assay to determine effects of CERS6 overexpression in SK-LC-5 cells. Two independent bulk clones were used. CERS6 expression levels are shown on top. (D) A549 cells were treated with mock, siCTRL, or siCERS6-1. Two days later, 1 x 10^6 cells were injected into tail veins (n=8). Three weeks after injection, the mice were euthanized to analyze lung metastasis. Left, representative lung samples are shown. Bar, 5 mm. Right, the number of metastasis sites was quantitated. *p* values were calculated using a two tailed t test.

Supplementary Fig. 6

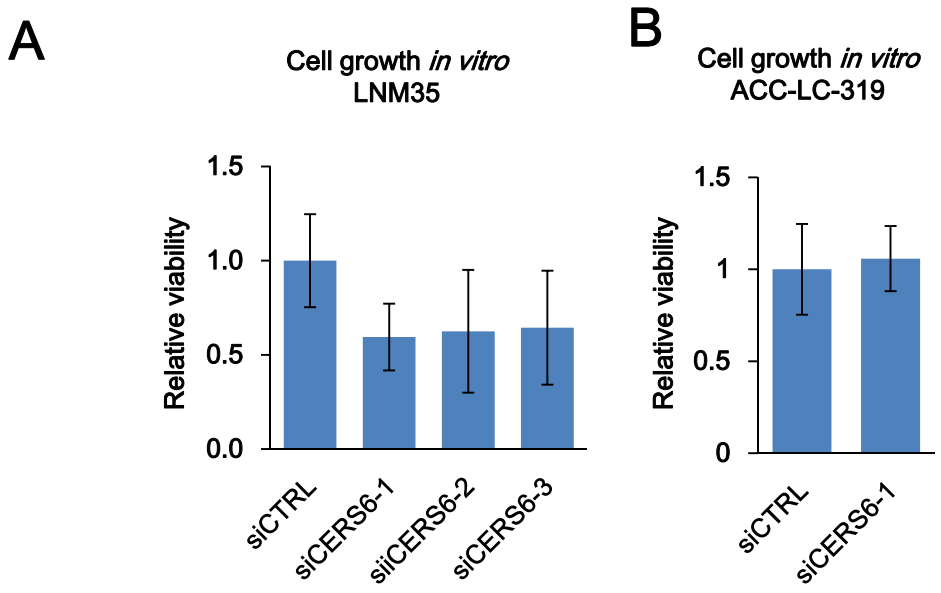

CERS6 knockdown or overexpression shows marginal effects on cell proliferation.
Five hours after LNM35 (A) or ACC-LC-319 (B) cells were treated with either 10 nM siCTRL or siCERS6-1~3, the culture medium was replaced with RPMI supplemented with EGF and N2 supplement. Cell viability was measured 48 hours after siRNA treatment. Bars, mean±SD (n=6).

Supplementary Fig. 7

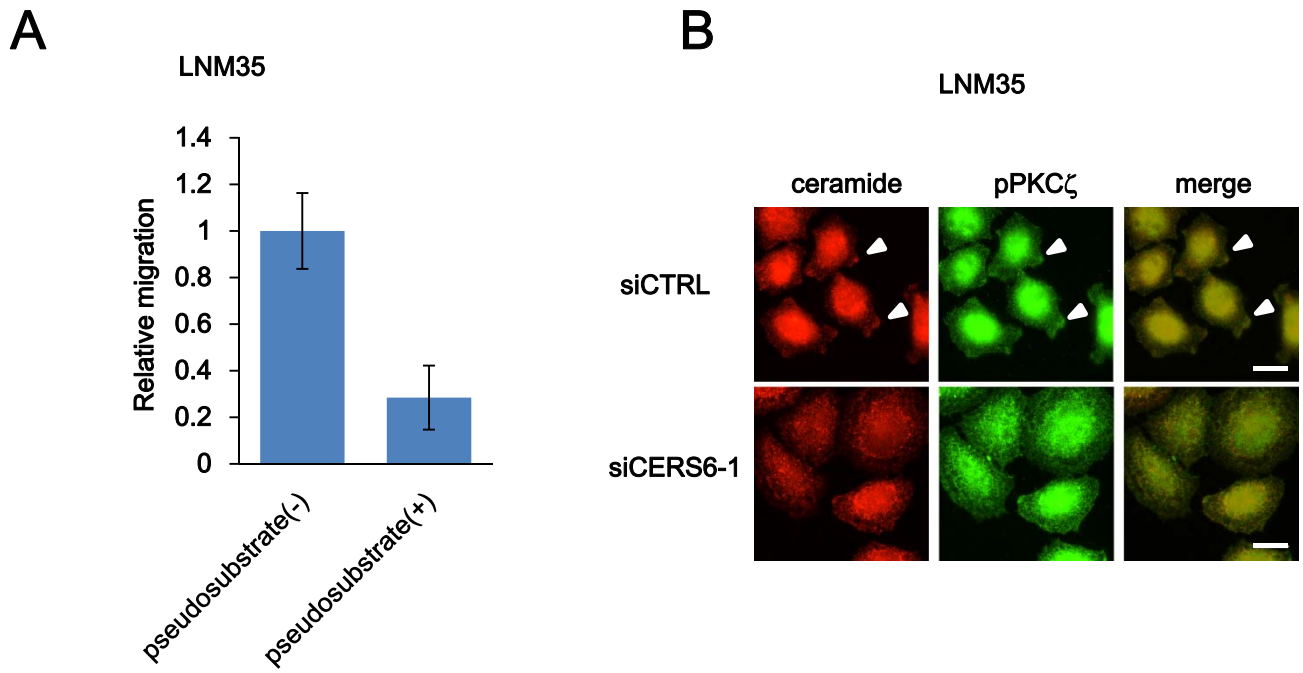

C16:0 ceramide may stimulate lamellipodia/ruffling formation through PKCζ activation.
(A) Migration assays were performed in the presence or absence of 1 μM PKCζ pseudo-substrate (Calbiochem). (B) Twelve hours after serum stimulation, cells were fixed and stained by anti-ceramide and anti-pPKCζ antibodies. Bar, 10 μm.

Supplementary Fig. 8

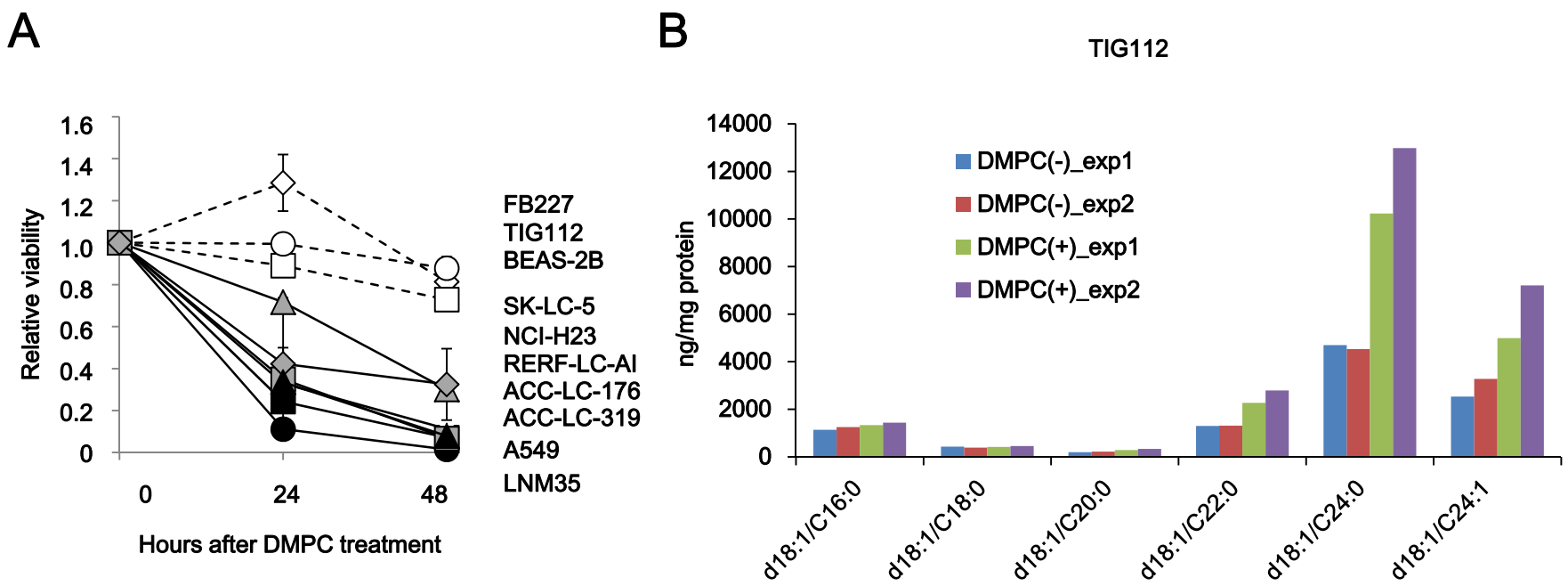

Effects of DMPC liposome on cell survival in types of cell lines.
(A) MTT assays were performed for determining the viability of a panel of cell lines (ACC-LC-176, BEAS-2B, SK-LC-5, RERF-LC-AI, NCI-H23, A549, ACC-LC-176, LNM35, FB227, TIG112) after treatment with 200 μM DMPC liposome. Data are shown as the mean ± SD (n=3~8). (B) Eight hours after DMPC treatment (200 μM), TIG112 cells were harvested and LCMS–IT–TOF mass spectrometry analysis was performed to quantify ceramide content. Results of duplicate experiments are shown.

Supplementary Fig. 9

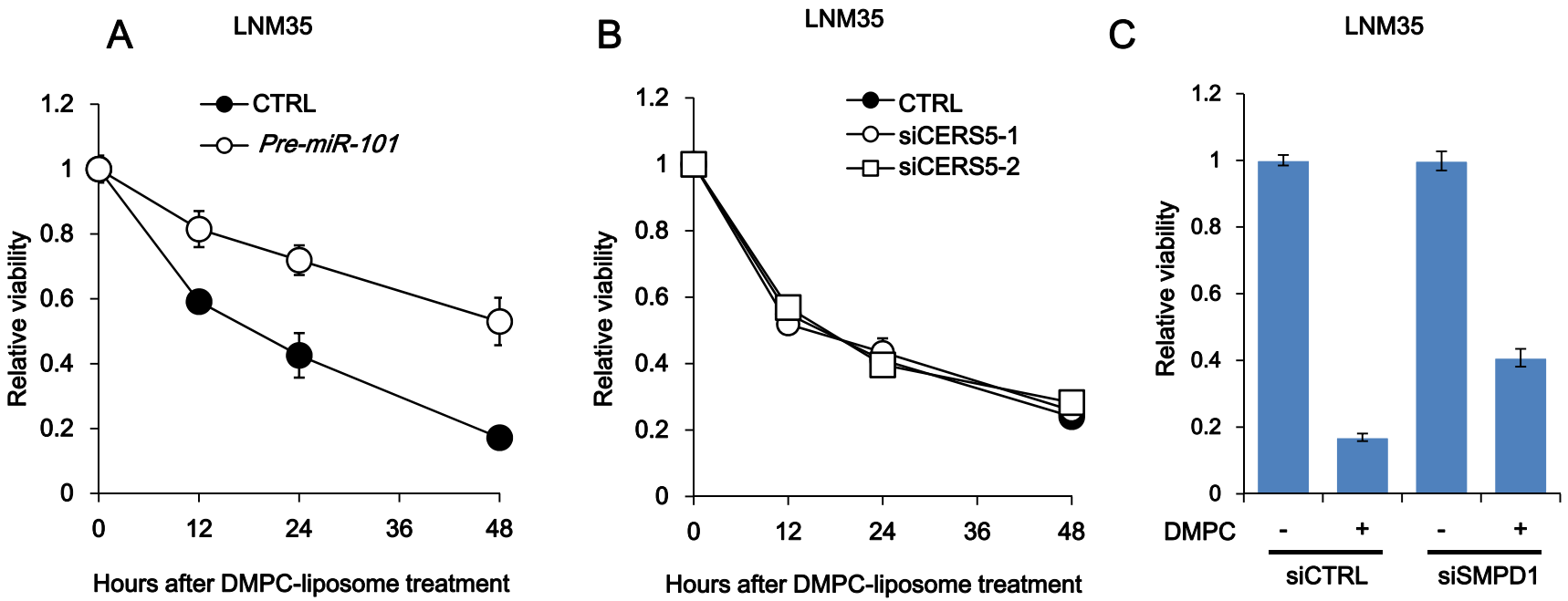

***miR-101* silencing attenuates apoptosis induced by DMPC liposome.**

(A) LNM35 cells were transfected with 1 nM CTRL or *pre-miR-101* for 48 hours, then further cultured with 100 μM DMPC-liposome for 48 hours and viability was determined. Bars, mean ± SD (n=3). (B) LNM35 cells were transfected with 20 nM siCERS5-1 or siCERS5-2 for 48 hours, then further cultured with 100 μM DMPC-liposome for 48 hours and viability was determined. Bars, mean ± SD (n=3). (C) LNM35 cells were transfected with 20 nM siSMPD1 for 48 hours, then further cultured with 100 μM DMPC-liposome for 48 hours and viability was determined. Bars, mean ± SD (n=3).

Supplementary Fig. 10

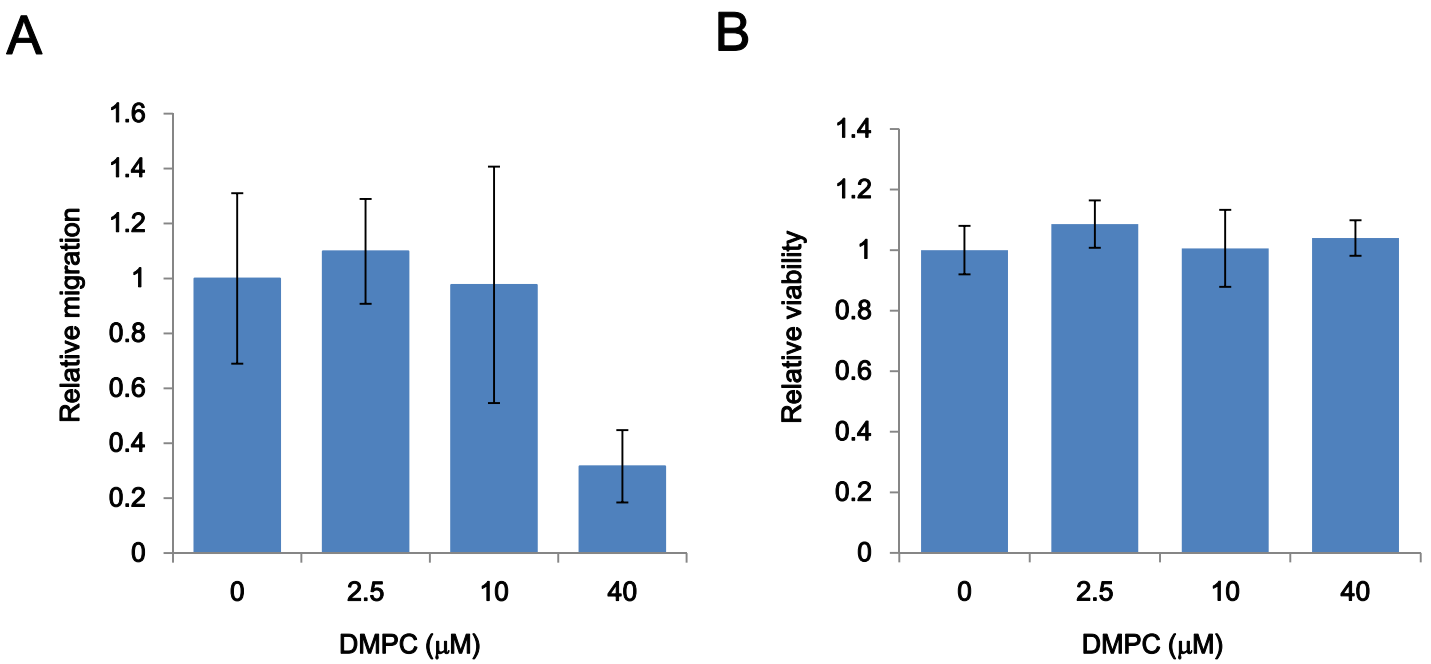

Migration activity of LNM35 under sub-lethal DMPC concentrations.
(A) Cell migration assays were performed to determine the effects of 0-40 μM DMPC in LNM cells. Bars, mean ± SD (n=4). (B) Cell viability assays were performed to determine the effects of the various levels of DMPC. Bars, mean ± SD (n=8).

Supplementary Fig. 11

A

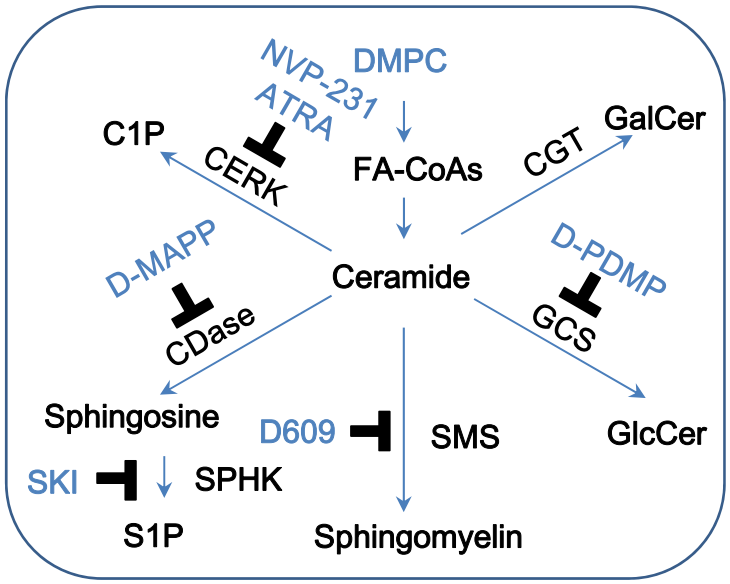

B

Co-effects of DMPC liposomes and D-PDMP derivatives

	IC_{50} (μM)
D-PDMP	
IC50($DMPC_{0\ \mu M}$) [μM]	20.6 ± 1.7
IC50($DMPC_{25\ \mu M}$) [μM]	8.7 ± 0.6
IC50($DMPC_{40\ \mu M}$) [μM]	6.3 ± 0.6
D-PMMP	
IC50($DMPC_{0\ \mu M}$) [μM]	13.7 ± 2.4
IC50($DMPC_{25\ \mu M}$) [μM]	7.1 ± 0.5
IC50($DMPC_{40\ \mu M}$) [μM]	4.1 ± 0.3
D-PPMP	
IC50($DMPC_{0\ \mu M}$) [μM]	8.5 ± 1.1
IC50($DMPC_{25\ \mu M}$) [μM]	4.4 ± 0.8
IC50($DMPC_{40\ \mu M}$) [μM]	1.9 ± 0.1

C

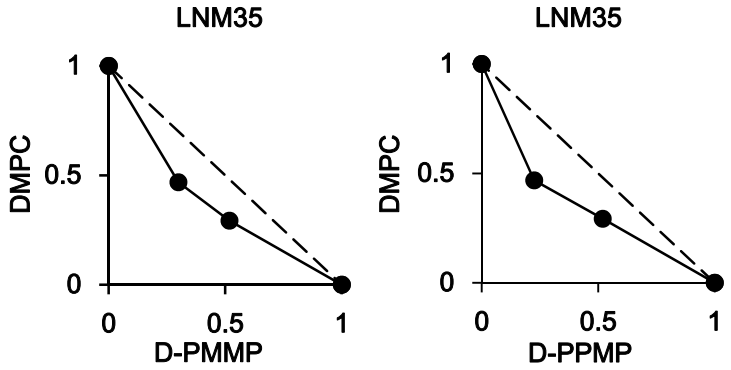

D

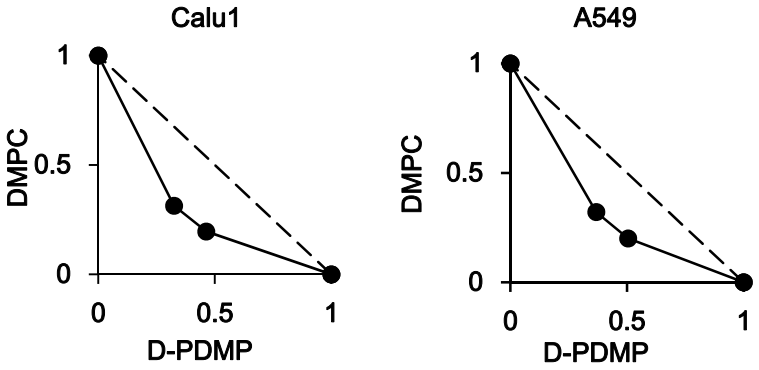

DMPC liposome and D-PDMP derivatives show synergistic effects in cancer cells.
(A) Overview of ceramide pathway inhibitors. NVP-231, ceramide kinase (CERK) inhibitor; D609, sphingomyelin synthase (SMS) inhibitor; SKI, sphingosine kinase (SPHK) inhibitor; D-MAPP, ceramidase (CDase) inhibitor; D-PDMP, glucosylceramide synthase (GCS) inhibitor. Note that ATRA transcriptionally suppressed ceramide kinase expression (J Neurochem 2010;112:511-520). (B) The co-effects of DMPC liposome and D-PDMP derivatives were determined in LNM35 cells. (C) Isobologram analyses of D-PDMP derivatives D-PMMP (left) and D-PPMP (right) in LNM35 cells. Horizontal and vertical axes show relative concentrations in D-PDMP derivatives and DMPC liposome, respectively. (D) Isobologram analyses of DMPC and D-PDMP in Calu1 and A549 cells.

Supplementary Fig. 12

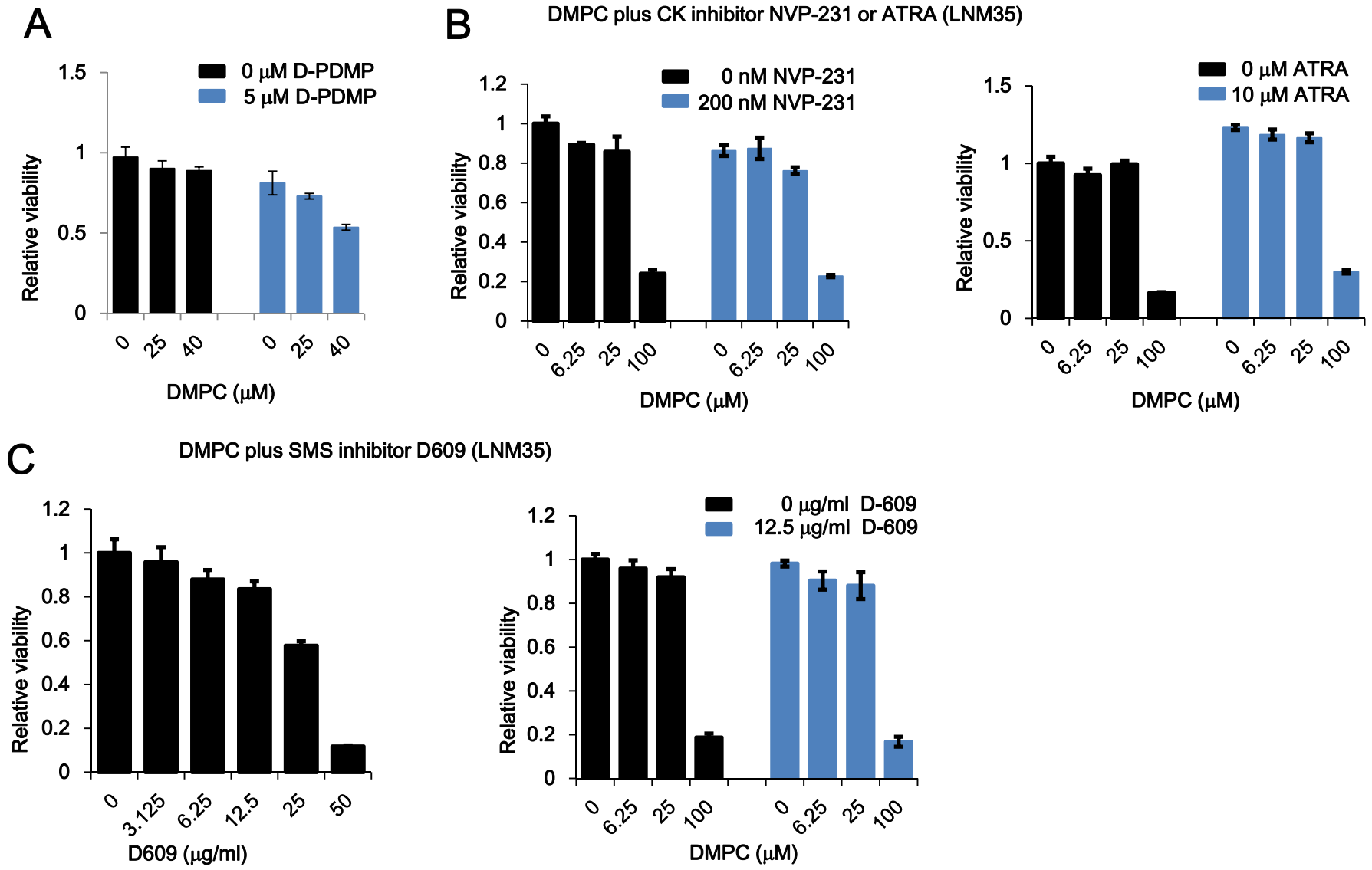

Effects of D-PDMP, CKI or SMS inhibitor combined with DMPC liposome.
(A) Cell viability assays for LNM35 cells treated with various concentrations of DMPC liposome with or without 5 μM D-PDMP. Bars, mean ± SD (n=4). (B) Cell viability assays for LNM35 cells treated with various concentrations of DMPC liposome with or without 200 nM NVP-231 or 10 μM ATRA. Bars, mean ± SD (n=3). (C) Cell viability assays for LNM35 cells treated with various concentrations of D609 (left). DMPC liposome concentrations varied with or without 12.5 μg/ml D609 (right). Bars, mean ± SD (n=3).

Supplementary Fig. 13

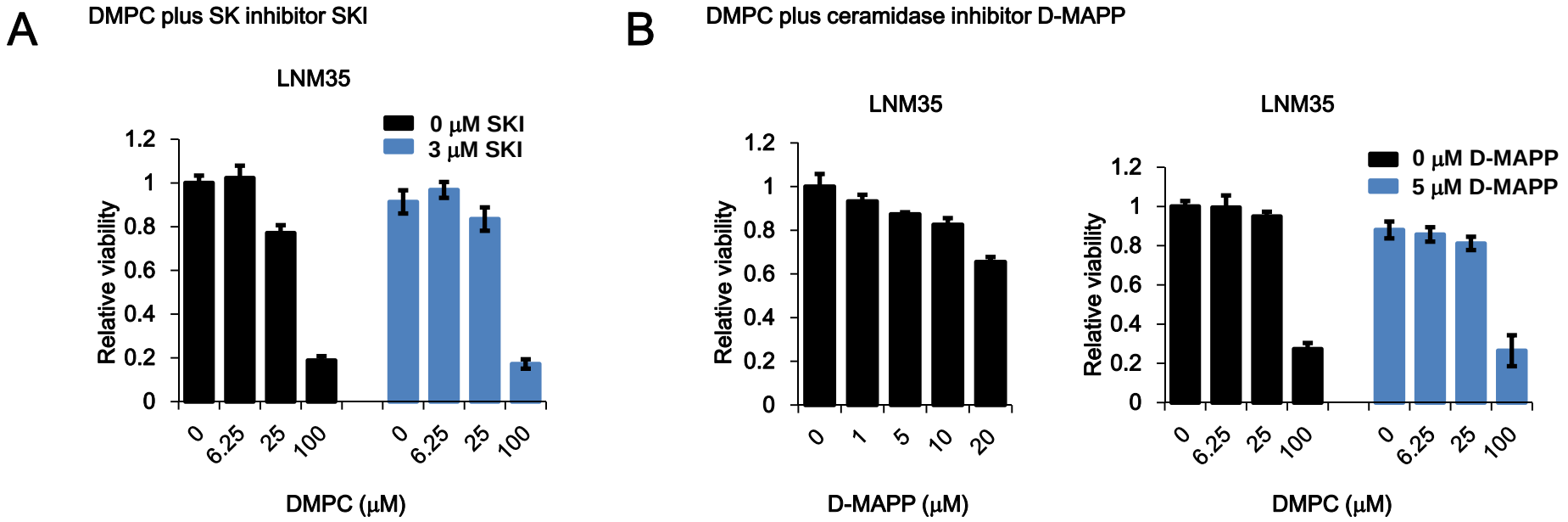

Effect of SKI or D-MAPP combined with DMPC liposome

(A) Cell viability assays for LNM35 cells treated with various concentrations of DMPC with or without 3 μM SKI. Bars, mean ± SD (n=3). (B) Cell viability assays for LNM35 cells treated with various concentrations of D-MAPP (left). DMPC liposome concentrations varied with or without 5 μM D-MAPP. Bars, mean ± SD (n=3).

Supplementary Fig. 14

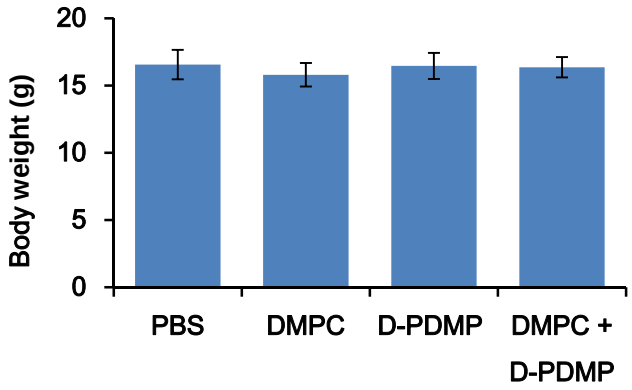

Effects of DMPC liposomes and D-PDMP on body weights.
After 200 μl of 50 mM DMPC and 2 mM D-PDMP were locally injected for 7 consecutive days, body weight was measured (n=5).